MOLECULAR ONCOLOGY 10 (2016) 360–370

available at www.sciencedirect.com

ScienceDirect

www.elsevier.com/locate/molonc

Targeted capture massively parallel sequencing analysis of LCIS and invasive lobular cancer: Repertoire of somatic genetic alterations and clonal relationships

Rita A. Sakr[a], Michail Schizas[a], Jose V. Scarpa Carniello[a], Charlotte K.Y. Ng[b], Salvatore Piscuoglio[b], Dilip Giri[b], Victor P. Andrade[a], Marina De Brot[a], Raymond S. Lim[b], Russell Towers[a], Britta Weigelt[b], Jorge S. Reis-Filho[b,c,**,1], Tari A. King[a,*,1]

[a]Breast Service, Department of Surgery, Memorial Sloan Kettering Cancer Center, New York, NY, United States
[b]Department of Pathology, Memorial Sloan Kettering Cancer Center, New York, NY, United States
[c]Human Oncology and Pathogenesis Program, Memorial Sloan Kettering Cancer Center, New York, NY, United States

ARTICLE INFO

Article history:
Received 24 July 2015
Received in revised form
9 October 2015
Accepted 3 November 2015
Available online 14 November 2015

Keywords:
Massively parallel sequencing
Invasive lobular carcinoma
Lobular carcinoma *in situ*
Clonality
Somatic genetic alterations

ABSTRACT

Purpose: Lobular carcinoma *in situ* (LCIS) has been proposed as a non-obligate precursor of invasive lobular carcinoma (ILC). Here we sought to define the repertoire of somatic genetic alterations in pure LCIS and in synchronous LCIS and ILC using targeted massively parallel sequencing.

Methods: DNA samples extracted from microdissected LCIS, ILC and matched normal breast tissue or peripheral blood from 30 patients were subjected to massively parallel sequencing targeting all exons of 273 genes, including the genes most frequently mutated in breast cancer and DNA repair-related genes. Single nucleotide variants and insertions and deletions were identified using state-of-the-art bioinformatics approaches.

Results: The constellation of somatic mutations found in LCIS (n = 34) and ILC (n = 21) were similar, with the most frequently mutated genes being *CDH1* (56% and 66%, respectively), *PIK3CA* (41% and 52%, respectively) and *CBFB* (12% and 19%, respectively). Among 19 LCIS and ILC synchronous pairs, 14 (74%) had at least one identical mutation in common, including identical *PIK3CA* and *CDH1* mutations. Paired analysis of independent foci of LCIS from 3 breasts revealed at least one common mutation in each of the 3 pairs (*CDH1*, *PIK3CA*, *CBFB* and *PKHD1L1*).

Conclusion: LCIS and ILC have a similar repertoire of somatic mutations, with *PIK3CA* and *CDH1* being the most frequently mutated genes. The presence of identical mutations

Abbreviations: LCIS, lobular carcinoma *in situ*; TCGA, The Cancer Genome Atlas; ILC, invasive lobular carcinoma; LOH, loss of heterozygosity; MSKCC, Memorial Sloan Kettering Cancer Center; H&E, hematoxylin and eosin; BWA, Burrows-Wheeler Aligner; GATK, Genome Analysis Toolkit; SNV, single nucleotide variant; indels, insertions and deletions; MAF, mutant allele fraction; MO, mutation occurrence; MR, mutation's rate of occurrence; PI, pair to be independent; ER, estrogen receptor.

* *Corresponding author.* Breast Service, Department of Surgery, Memorial Sloan Kettering Cancer Center, 300 E. 66th St., New York, NY 10065, United States. Tel.: +1 646 888 5352; fax: +1 212 794 5812.

** *Corresponding author.* Department of Pathology, Memorial Sloan Kettering Cancer Center, 1275 York Avenue, New York, NY 10065, United States. Tel.: +1 212 639 8054; fax: +1 212 639 2502.

E-mail addresses: reisfilj@mskcc.org (J.S. Reis-Filho), tking7@partners.org (T.A. King).

[1] J. S. Reis-Filho and T. A. King contributed equally to this article.

http://dx.doi.org/10.1016/j.molonc.2015.11.001

between LCIS–LCIS and LCIS–ILC pairs demonstrates that LCIS is a clonal neoplastic lesion, and provides additional evidence that at least some LCIS are non-obligate precursors of ILC.

1. Introduction

Lobular carcinoma *in situ* (LCIS) is a non-invasive neoplastic lesion of the breast characterized by expansion of the lobular units by a monomorphic population of dyscohesive cells. Most commonly identified as an incidental finding in otherwise benign breast biopsies, a diagnosis of LCIS confers one of the greatest risks currently recognized for the subsequent development of breast cancer. Yet the biology of this lesion and its potential for progression remain poorly understood. Hence, in clinical practice management, strategies following a diagnosis of LCIS vary widely from observation alone to bilateral prophylactic mastectomy (De Leeuw et al., 1997; Hwang et al., 2004; Lakhani et al., 2006; Vos et al., 1997).

Molecular studies based on the pattern of gene copy number alterations and *CDH1* mutations provide supporting evidence that LCIS likely constitutes a non-obligate precursor of invasive lobular carcinoma (ILC) (Andrade et al., 2012; Hwang et al., 2004; Lakhani et al., 1995; Vos et al., 1997). Our group and others have shown that synchronous LCIS and ILC share similar copy number aberrations, predominantly 16q loss and 1q gain (Andrade et al., 2012; Hwang et al., 2004; Lakhani et al., 1995). Historical studies have also demonstrated the presence of the same truncating mutations in the E-cadherin gene *CDH1* and loss of heterozygosity (LOH) of the wild-type allele in a small number of synchronous LCIS and ILC cases (Vos et al., 1997). An analysis of 36 ILCs included in the first genomic characterization of breast cancers by The Cancer Genome Atlas (TCGA) revealed that ILCs harbor a repertoire of somatic mutations similar to that of luminal cancers, but have a higher frequency of *CDH1* and *ERBB2* somatic mutations (Cancer Genome Atlas, 2012; Ciriello et al., 2015). To our knowledge, the repertoire of somatic mutations in LCIS has not been reported to date.

The advent of targeted capture massively parallel sequencing has made it possible to investigate somatic mutations from limited amounts of DNA (Wagle et al., 2012). The methodology allows for simultaneous identification of base substitutions, insertions/deletions, copy number aberrations and structural alterations with greater sensitivity and cost effectiveness than traditional sequencing methods. Here we describe the repertoire of genomic changes in fresh-frozen samples of LCIS with or without synchronous ILC subjected to targeted capture massively parallel sequencing of all exons of 273 genes, including the genes most recurrently mutated in breast cancer and genes related to DNA repair. Using this approach, we sought to define the repertoire of genetic alterations in LCIS and ILC, and to investigate the clonal relatedness of synchronous LCIS and ILC, and of multiple foci of LCIS.

2. Materials and methods

2.1. Patients and samples

Patients with a documented history of LCIS, presenting for prophylactic or therapeutic mastectomy, were identified preoperatively and enrolled in a Memorial Sloan Kettering Cancer Center (MSKCC) institutional review board-approved protocol for the collection of fresh-frozen tissue and genomic analyses (IRB 01-135). Following standard clinical sampling, mastectomy specimens were subject to random sampling, and up to 10 fresh-frozen blocks per quadrant were harvested and stored at −80 °C for subsequent analysis. For the purposes of this study, 5μm hematoxylin and eosin (H&E) frozen sections were reviewed by at least two study pathologists (DG, MDB, VPA) to identify blocks with LCIS, with or without invasive cancer. Histologic criteria for LCIS and ILC were those described by the 2012 World Health Organization classification (Lakhani S.R. EIO, 2012). Although some patients included in this study also had ductal lesions (invasive ductal cancer or ductal carcinoma *in situ*) identified on standard clinical pathology, only classic LCIS and ILC lesions harvested as part of protocol 01–135 were included in this study. Matched germline DNA from peripheral blood or normal breast tissue devoid of any neoplastic cells were available for all cases. All samples were anonymized prior to analysis.

2.2. Microdissection and DNA extraction

Sequential sections (15μm-thick) from selected frozen blocks were prepared for microdissection of *in situ* and/or invasive lesions using a stereomicroscope to ensure tumor cell enrichment, as previously described (Sakr et al., 2014). The number of sections used for microdissection varied based on lesion size and cellularity with an average of 35 sections per lesion (range 6–89). DNA was extracted from microdissected samples of LCIS, ILC and normal breast ducts using the QIAamp DNA Micro Kit (Qiagen, Valencia, CA) according to the manufacturer's instructions. Germline DNA was extracted from peripheral blood leukocytes using the QIAamp DNA Blood Maxi Kit (Qiagen). DNA was quantified using the Qubit Fluorometer (Life Technologies, Norwalk, CT).

2.3. Targeted capture massively parallel sequencing

Tumor and matched normal DNA obtained from 30 patients resulted in the availability of 85 samples (34 LCIS, 21 ILC, and 30 normal) for the purposes of this study (Table 1). Targeted capture massively parallel sequencing was performed on a platform containing baits for all exons of 273 genes recurrently

Table 1 – Distribution of the 34 LCIS and 21 ILC samples obtained from 30 patients included in this study.

	Number of patients	Same quadrant	Different quadrant
LCIS only	3	–	–
ILC only	6	–	–
LCIS – LCIS pair	6	1	5
LCIS – ILC pair	11	10	1
LCIS – LCIS – ILC triplet	4*	–	4

ILC, invasive lobular cancer; LCIS, lobular carcinoma *in situ*; *corresponding to 4 LCIS – LCIS pairs and 8 LCIS – ILC pairs.

mutated in breast cancer and involved in DNA repair pathways (Natrajan et al., 2014). Barcoded sequence libraries were prepared (New England Biolabs, Ipswich, MA; KapaBiosystems, Wilmington, MA) using at least 50ng of sheared DNA and pooled at equimolar concentrations into a single exon capture reaction (Roche NimbleGen, Madison, WI) (Cheng et al., 2015). Paired-end massively parallel sequencing was performed on a HiSeq2000 (Illumina, San Diego, CA).

Reads were aligned to the reference human genome GRCh37 using the Burrows-Wheeler Aligner (BWA) and sequencing data were processed by Genome Analysis Toolkit (GATK) (Li and Durbin, 2009; McKenna et al., 2010). Single nucleotide variants (SNVs) were defined using a combination of five mutation callers (i.e., MuTect, MutationSeq, GATK HaplotypeCaller, VarScan2 and SomaticSniper) (Cibulskis et al., 2013; Ding et al., 2012; Koboldt et al., 2012; Larson et al., 2012; McKenna et al., 2010). Small insertions and deletions (indels) were identified using the GATK HaplotypeCaller and VarScan2 (Koboldt et al., 2012; McKenna et al., 2010). Mutant allele fraction (MAF) was defined as the number of copies of the mutant allele divided by the number of copies of all alleles at a given locus. Mutations with allelic fraction of <5%, and/or those not detected by at least 2 of 5 mutation callers and not supported by at least 5 reads were disregarded. All candidate mutations were manually reviewed using the Integrative Genomics Viewer (Robinson et al., 2011). Copy number plots were generated using Varscan2, and were used for manual curation to determine whether a gene harboring a somatic mutation was also targeted by LOH.

Potential functional effect of each missense SNV was investigated using a combination of MutationTaster (Schwarz et al., 2010) and CHASM (Carter et al., 2009), and mutations identified as neutral/passengers by both computational prediction algorithms were considered passenger mutations, as previously described (Martelotto et al., 2014). The effect of in-frame indels was predicted using PROVEAN and MutationTaster (Choi et al., 2012; Schwarz et al., 2010). Genes affected by non-passenger mutations were further annotated using FATHMM (Shihab et al., 2013) and according to their presence in three cancer gene datasets: Cancer Gene Census (Futreal et al., 2004), 127 genes by Kandoth et al. (Kandoth et al., 2013) and the Cancer-5000S dataset by Lawrence et al. (Lawrence et al., 2014). "Lollipop plots" showing the distribution of mutations were generated using MutationMapper on cBioPortal (http://www.cbioportal.org/public-portal/mutation_mapper.jsp) (Gao et al., 2013).

2.4. *Mutation validation*

Samples with hotspot *PIK3CA* mutations and residual DNA were subjected to Sequenom MassARRAY (Sequenom) for validation of the *PIK3CA* mutations as previously described (Chandarlapaty et al., 2012; Sakr et al., 2014). Residual DNA from samples with *CDH1* mutations were subjected to Sanger sequencing with primer sets (5′-CTGGGGTCCTCCCCAAT-3' (forward), 5′-GGTGTGGGAGTGCAATTTCT-3' (reverse)) as previously described (Weinreb et al., 2014). All analyses were performed in duplicate. Sequences of the forward and reverse strands were analyzed using MacVector software (MacVector, Inc, Cary, NC) (Weinreb et al., 2014).

2.5. *Clonality analysis*

To infer clonal relatedness between lesions, we calculated for each mutation the probability of the mutation occurring in a pair of samples independently. Given that TCGA samples are unrelated, we chose to calculate each mutation's rate of occurrence in the luminal-A subset of 235 samples (Cancer Genome Atlas, 2012): Mutation occurrence (MO) = number of mutations/235 samples; Mutation's rate of occurrence (MR) = MO × 100. The resulting probability of a pair to be independent (PI) based solely on that mutation would be the square of the mutation's rate of occurrence in the mentioned subset: PI = MR × MR. Subsequently, we derived the probability of a pair to be clonal (PC) based on that mutation, by deducting the probability of a pair to be independent from 100: PC = 100 − PI. The total clonality confidence call is then the product of all shared mutations' probability of clonality (PC): TPC = PC1 × PC2 × … × PCn (n = number of shared mutations). To further assess relatedness, we also performed unsupervised hierarchical clustering (Ward's clustering algorithm with Euclidean distance) of samples harboring recurrent non-synonymous SNVs, silent SNVs and indels. We defined a recurrent SNV or indel as one that occurred in at least two samples.

2.6. *Statistical analysis*

Comparisons were assessed using Fisher's exact and Chi-Square tests. 95% confidence intervals were adopted and p-values <0.05 were considered significant. Statistical analyses were performed using SAS software, version 9.1 (SAS Institute, Cary, NC).

3. Results

Fresh-frozen tissue samples were prospectively harvested from 3 patients undergoing prophylactic mastectomy and 27 patients undergoing therapeutic mastectomy for ILC. From these 30 patients, we obtained DNA from 34 samples of LCIS and 21 samples of ILC (Table 1). This included 6 patients with paired LCIS samples (LCIS–LCIS), 11 patients with paired LCIS–ILC samples and 4 patients with triplets (2 LCIS and 1 ILC) resulting in a total of 19 LCIS–ILC comparisons and 10 LCIS–LCIS comparisons in the pairwise analysis. Selected samples from 4 cases reported here were also included in a

parallel whole-exome sequencing analysis performed by our laboratory (Table 2, Table 3). The average size of the ILC lesions was 24 mm (range 14–75), and 26/26 (100%) of the ILC were estrogen receptor (ER)-positive/HER2-negative (Supplementary Table S1). ER and HER2 status were not assessed on the individual foci of LCIS. All LCIS and ILC lesions were E-cadherin negative by immunohistochemistry.

3.1. *Targeted capture massively parallel sequencing analysis of LCIS*

LCIS samples were sequenced to a median target depth of 238× (range 75×–603×), which resulted in the identification of 96 somatic mutations affecting 53 (19%) of the 273 genes analyzed. Of the LCIS samples analyzed, 82% (28/34) harbored at least one somatic mutation, and 68% (23/34) harbored two or more mutations. Of the 96 detected mutations, 66 (69%) were non-synonymous SNVs, 19 (20%) were indels and 11 (11%) were silent mutations. Genes recurrently affected by non-synonymous mutations in LCIS included *CDH1*, *PIK3CA* and *CBFB* with mutation frequencies of 56%, 41% and 12%, respectively (Figure 1, Supplementary Table S2). *CDH1* gene mutations included 10 non-synonymous SNVs (10 splice-site) and 9 indels (8 frameshift, 1 splice-site) distributed among the multiple domains of the gene (Supplementary Fig. S1); all *CDH1* mutations were considered likely non-passenger events (Supplementary Table S3). LOH of 16q with *CDH1* mutation was observed in 18/19 samples (Supplementary Table S3). *PIK3CA* gene mutations identified in LCIS included 15 non-synonymous SNVs (all missense) and 1 indel, of which 8 were found in the kinase domain (5 H1047R, 2 H1047L, 1 D1029H) and 5 in the helical domain (2 E542K, 1 E545K, 1 E545G, 1 Q546R); all mutations outside the helical and kinase domains (1 N345K, 1 D350N) and the indel (E110del) also outside the helical and kinase domains were considered to be non-passenger events (Supplementary Table S3); however, the biological impact of the indel identified remains to be determined. *CBFB* gene mutations included 3 non-synonymous SNVs (all missense) and 1 indel (splice-site), all considered to be non-passenger (Supplementary Table S3). LOH with *CBFB* mutation was observed in all 4 samples (Supplementary Table S3).

Among the 3 patients who underwent prophylactic mastectomy, there were 5 LCIS samples, of which one sample harbored a single mutation in the *MAP3K1* (I1440T) gene and one sample displayed a mutation in *CDH1* (H632fs), *ERBB2* (L755S) and *LAMA5* (P1241Q) (Supplementary Tables S3 and S4). All mutations except the *LAMA5* mutation were considered to be likely non-passenger events (Supplementary Table S3).

PIK3CA mutations (H1047R, H1047L, E542K, D350N) in 8 LCIS samples with available residual DNA were confirmed by Sequenom analysis, and *CDH1* mutation (Q23*) in 3 LCIS samples with available residual DNA was confirmed by Sanger sequencing analysis (Supplementary Table S3).

3.2. *Targeted capture massively parallel sequencing analysis of ILC*

ILC samples were sequenced to a median target depth of 307× (range 55×–665×), which resulted in the identification of 113 somatic mutations (80 non-synonymous SNVs, 12 indels and 21 silent mutations) involving 71 (26%) of the 273 genes analyzed. At least one non-synonymous mutation was identified in 19 (90%) samples and two or more non-synonymous mutations were found in 17 (81%) samples. As in LCIS samples, the genes recurrently affected by non-synonymous mutations were *CDH1*, *PIK3CA* and *CBFB* with mutation frequencies of 66%, 52% and 19%, respectively (Figure 1, Supplementary Table S2). *CDH1* gene mutations included 8 non-synonymous SNVs (6 nonsense and 2 splice-site) and 6 indels (5 frameshift and 1 splice-site); all *CDH1* mutations were considered likely non-passenger events (Supplementary Table S3). These 14 samples harboring *CDH1* somatic mutations concurrently harbored LOH of the *CDH1* wild-type allele. *PIK3CA* gene mutations included 11 non-synonymous SNVs (all missense) and 1 indel (E109del), with 4 mutations found in the kinase domain (3 H1047R, 1 H1047L) and 4 in the helical domain (1 E542K, 3 E545K). All *PIK3CA* mutations were considered non-passenger events (Supplementary Table S3). *CBFB* gene mutations included 4 non-synonymous SNVs, all missense and considered to be non-passenger events (Supplementary Table S3). LOH with *CBFB* mutation was observed in all 4 samples (Supplementary Table S3).

PIK3CA mutations (H1047R, H1047L, E545K, E542K, N345K) in 9 ILC samples with available residual DNA were confirmed by Sequenom analysis and *CDH1* mutation (Q23*) in 2 ILC samples with available residual DNA was confirmed by Sanger sequencing analysis (Supplementary Table S3).

3.3. *Comparison of the repertoire of somatic genetic alterations in LCIS and ILC*

To define the differences in the repertoire of somatic genetic alterations found in LCIS and ILC, we first identified the genes commonly mutated between the LCIS and ILC analyzed. 30 genes were found to be affected by somatic mutations in both LCIS and ILC, including many genes reported to be recurrently mutated in ER-positive/luminal breast cancers (e.g., *CDH1*, *ERBB3*, *GATA3*, *FOXA1*, *PIK3CA*, *MAP3K1*, *RUNX1*, *TP53*, *PTEN*) (Banerji et al., 2012; Cancer Genome Atlas, 2012; Ellis et al., 2012; Stephens et al., 2012).

A comparison of the recurrently mutated genes in ILC and LCIS revealed no statistically significant difference between LCIS and ILC for any of the individual genes (Fisher's exact test, $p > 0.5$; Supplementary Table S2, Figure 1). Taken together, these findings demonstrate that LCIS and ILC harbor similar constellations of somatic mutations.

3.4. *The majority of synchronous LCIS and ILC and independent ipsilateral foci of LCIS are clonally related*

Pairwise analysis of the 19 LCIS–ILC paired lesions demonstrated at least one shared mutation in 14 (74%) sample pairs (Table 2). Among these 14 pairs, 7 LCIS–ILC pairs shared both identical *CDH1* and *PIK3CA* mutations, 5 LCIS–ILC pairs shared a *CDH1* mutation, and 1 LCIS–ILC pair shared a *PIK3CA* mutation. The analysis of the probability of a pair to be clonal based on number of shared mutations revealed that all 14 LCIS–ILC pairs were clonal, with a clonality confidence between 97% and 99.9% (Supplementary Table S5). Unsupervised

Table 2 – Shared mutations identified in pairs of LCIS – ILC lesions.

Case number	Lesion	Side-Quadrant	*CDH1*	*PIK3CA*	*CBFB*	*PKHD1L1*	*RUNX1*	*MAP3K1*	*CDC25B*	*RELN*	*HERC2*	*PCNXL2*	*PDGFRA*	*ABCA13*
10	LCIS1¥	R-UOQ	Q23* (21%)	H1047L (22%)	V4L (27%)	–	–	–	–	–	–	–	–	–
	ILC¥	R-UOQ	Q23* (34%)	H1047L (20%)	V4L (16%)	–	–	–	–	–	–	–	–	–
	LCIS2	R-UIQ	Q23* (18%)	H1047L (22%)	V4L (19%)	–	–	–	–	–	–	–	–	–
	ILC	R-UOQ	Q23* (34%)	H1047L (20%)	V4L (16%)	–	–	–	–	–	–	–	–	–
13	LCIS1	L-UOQ	E336_splice (25%)	–	–	V1686I (17%)	–	–	–	–	–	–	–	–
	ILC	L-UIQ	E336_splice (11%)	–	–	V1686I (16%)	–	–	–	–	–	–	–	–
	LCIS2	L-LOQ	E336_splice (7%)	–	–	V1686I (10%)	–	–	–	–	–	–	–	–
	ILC	L-UIQ	E336_splice (11%)	–	–	V1686I (16%)	–	–	–	–	–	–	–	–
24	LCIS1¥ϕ	R-LOQ	F730fs (17%)	H1047R (20%)	Q67H (26%)	–	–	–	–	–	–	–	–	–
	ILC¥ϕ	R-LOQ	F730fs (10%)	H1047R (12%)	Q67H (20%)	–	–	–	–	–	–	–	–	–
28	LCIS¥	L-UIQ	D367fs (33%)	–	–	–	L71fs (29%)	–	–	–	–	–	–	–
	ILC¥	L-UIQ	D367fs (61%)	–	–	–	L71fs (36%)	–	–	–	–	–	–	–
29	LCIS¥	R-LIQ	Q23* (29%)	N345K (16%)	–	–	–	S416* (7%)	–	–	–	–	–	–
	ILC¥	R-LIQ	Q23* (48%)	N345K (28%)	–	–	–	S416* (16%)	–	–	–	–	–	–
31	LCIS¥	L-UOQ	E547* (35%)	–	–	–	–	–	R175Q (24%)	–	–	–	–	–
	ILC¥	L-UOQ	E547* (54%)	–	–	–	–	–	R175Q (33%)	–	–	–	–	–
33	LCIS¥	R-UOQ	–	–	–	–	–	–	–	–	–	R1215W (11%)	–	–
	ILC¥	R-UOQ	–	–	–	–	–	–	–	–	–	R1215W (14%)	–	–
38	LCIS¥ϕ	R-UOQ	522_splice (16%)	D350N (10%) E545K (15%)	–	–	–	–	–	–	–	–	E289K (15%)	Q4805Q (14%)
	ILC¥ϕ	R-UOQ	522_splice (10%)	D350N (16%) E545K (20%)	–	–	–	–	–	–	–	–	E289K (13%)	Q4805Q (9%)
48	LCIS1¥ϕ	L-UOQ	571_splice (56%)	–	–	–	–	–	–	–	–	–	–	–
	ILC¥ϕ	L-UOQ	571_splice (32%)	–	–	–	–	–	–	–	–	–	–	–
52	LCIS¥	R-UOQ	I248fs (21%)	H1047R (14%)	–	–	–	–	–	–	–	–	–	–
	ILC¥	R-UOQ	I248fs (22%)	H1047R (17%)	–	–	–	–	–	–	–	–	–	–
54	LCIS¥	L-UOQ	L714fs (6%)	E542K (13%)	–	–	–	–	–	–	R3668Q (14%)	–	–	–
	ILC¥	L-UOQ	L714fs (6%)	E542K (15%)	–	–	–	–	–	–	R3668Q (17%)	–	–	–
55	LCIS¥	R-UOQ	–	H1047R (19%)	–	–	–	–	–	T429S (20%)	–	–	–	–
	ILC¥	R-UOQ	–	H1047R (18%)	–	–	–	–	–	T429S (16%)	–	–	–	–

ILC, invasive lobular cancer; L, left side; LCIS, lobular carcinoma *in situ*; LIQ, lower inner quadrant; LOQ, lower outer quadrant; MAF, mutant allele fraction; R, right side; UIQ, upper inner quadrant; UOQ, upper outer quadrant; ¥ same quadrant; ϕ samples also subjected to whole-exome sequencing. For each gene/mutation, the amino acid change and the mutant allele fraction are shown. Shared mutations were identified in 14/19 pairs of LCIS–ILC.

Table 3 – Shared mutations identified in pairs of LCIS – LCIS lesions.

Case number	Lesion	Side-Quadrant	*CDH1*	*PIK3CA*	*CBFB*	*PKHD1L1*
10	LCIS-1	R-UOQ	Q23* (21%)	H1047L (22%)	V4L (27%)	–
	LCIS-2	R-UIQ	Q23* (18%)	H1047L (22%)	V4L (19%)	–
13	LCIS-1	L-UOQ	E336_splice (25%)	–	–	V1686I (17%)
	LCIS-2	L-LOQ	E336_splice (7%)	–	–	V1686I (10%)
53	LCIS-1[¥ϕ]	R-UIQ	I178_splice (25%)	–	–	–
	LCIS-2[¥ϕ]	R-UIQ	I178_splice (7%)	–	–	–

ILC, invasive lobular cancer; L, left side; LCIS, lobular carcinoma *in situ*; LIQ, lower inner quadrant; LOQ, lower outer quadrant; MAF, mutant allele fraction; R, right side; UIQ, upper inner quadrant; UOQ, upper outer quadrant; [¥] same quadrant; [ϕ] samples also subjected to whole-exome sequencing. For each gene/mutation, the amino acid change and the mutant allele fraction are shown. Shared mutations were identified in 3/10 pairs of LCIS-LCIS.

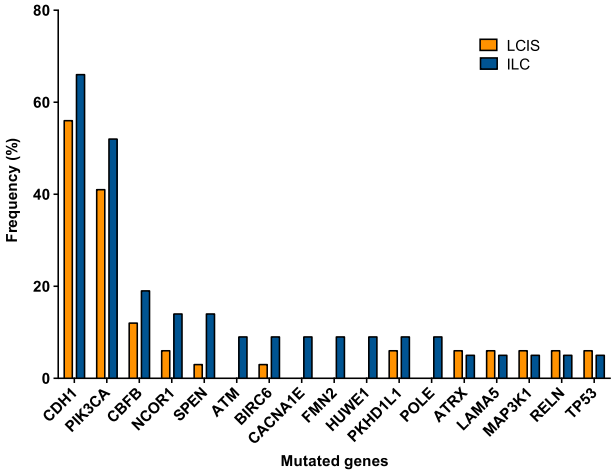

Figure 1 – Mutational frequency of recurrently mutated genes in LCIS and ILC lesions. Recurrently mutated genes identified by targeted massively parallel sequencing in 34 LCIS (orange) and 21 ILC (blue) analyzed in this study. ILC, invasive lobular carcinoma; LCIS, lobular carcinoma *in situ*.

hierarchical clustering of all LCIS and ILC samples included in this study using the most recurrently mutated genes (Figure 2) revealed that the 14 matched LCIS–ILC preferentially clustered together (13/14 pairs clustered together), providing additional evidence for the relatedness of these LCIS–ILC pairs. Anatomically, the paired lesions included in this study were located in the same quadrant of the breast in the majority of cases (11/14, 79% of LCIS–ILC pairs), and three pairs were located in different quadrants of the breast, the latter being derived from patients who underwent therapeutic mastectomy.

In three LCIS–ILC pairs, distinct mutations were observed in LCIS and ILC samples. In the first case (Case #03), the paired lesions were located in the same quadrant of the breast; however, the ILC harbored a *PIK3CA* and a *PIK3R1* mutation, whereas the LCIS harbored a *PTEN* mutation (Figure 3). In the second case (Case #48), the lesions were located in different quadrants of the breast; whilst the ILC and LCIS-1 in the same quadrant harbored an identical *CDH1* splice-site mutation, the LCIS-2 in a different quadrant harbored an *ATRX* mutation instead. In the third case (Case #24), we found that the ILC harbored a *CDH1* (F730fs) and *PIK3CA* (H1047R) mutation distinct from those found in the LCIS-2 lesion in a different quadrant (*CDH1* Q23*; *PIK3CA* Q546R). Furthermore, a *CBFB* mutation was found to be restricted to the ILC, while *GATA3*, *HMNC1*, *MAP4K4*, and *MLL3* mutations were unique to the LCIS-2 lesion (Figure 3).

The remaining 2 LCIS–ILC pairs tested were equivocal with no mutations detected in one or both lesions of the pair (Supplementary Table S6).

We also compared multiple foci of LCIS from the same patient. Of the 10 LCIS–LCIS pairs included in this study, 3 (30%) pairs showed at least one common mutation (Table 3). The two LCIS lesions of the first pair (Case #53) were located in the same quadrant of the breast and shared an identical *CDH1* I178 splice-site mutation. The second and third pairs were located in different quadrants of the breast and shared 2 (*CDH1* and *PKHD1L1*) and 3 (*CDH1*, *PIK3CA* and *CBFB*) identical mutations, respectively (Table 3). The analysis of the probability of a LCIS–LCIS pair to be clonal based on the number of shared mutations revealed that all 3 cases the LCIS lesions were likely clonal with a clonality confidence between 98% and 99.9% (Supplementary Table S5). This was further supported by the observation that these 3 LCIS–LCIS pairs clustered together in the unsupervised hierarchical clustering performed (Figure 2 and Supplementary Fig. S2). Conversely, distinct mutations were observed in 4 (40%) LCIS–LCIS pairs; in these pairs, the LCIS lesions were located in different quadrants of the breast. The remaining 3 (30%) LCIS–LCIS pairs were equivocal due to the lack of mutations in one or both of the lesions of the pair (Supplementary Table S6).

Overall, among all 17 LCIS–ILC or LCIS–LCIS pairs inferred to be clonal based on the number of shared mutations and unsupervised hierarchical clustering, 12 (71%) were located in the same quadrant of the breast, whereas 5 (29%) were found in

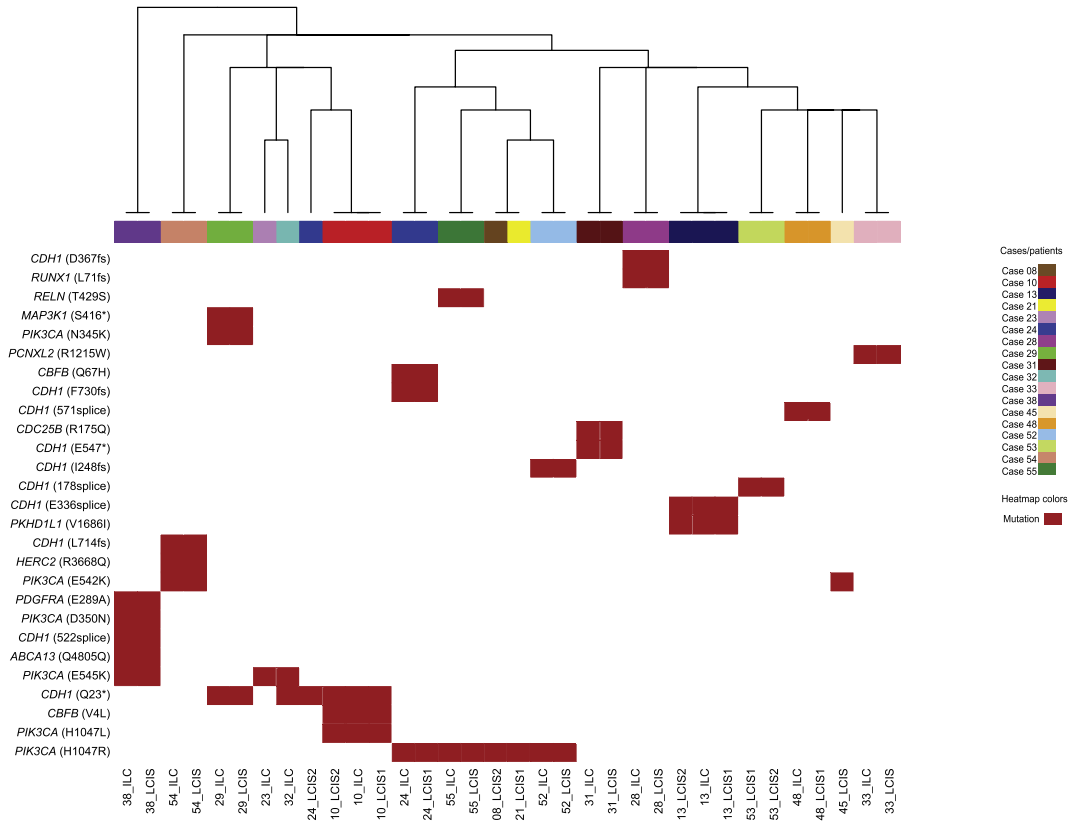

Figure 2 – Unsupervised hierarchical clustering of LCIS and ILC samples using the recurrent somatic mutations identified by targeted massively parallel sequencing. Hierarchical clustering of recurrent mutations identified in LCIS and ILC samples. Hierarchical cluster analysis was performed using Ward's clustering algorithm with Euclidean distance. The colors in the phenobar represent lesions of a given case; the red box represents the presence of a mutation. Note that all paired LCIS–ILC samples cluster together. ILC, invasive lobular carcinoma; LCIS, lobular carcinoma *in situ*.

different quadrants (Fisher's exact test, 71% vs 29%, $p = 0.038$). Of the 7 pairs determined to be non-clonal based on the presence of distinct mutations, 1 pair (case #03) was located in the same quadrant of the breast and 6 were in different quadrants of the breast (Fisher's exact test, 16% vs 86%, $p = 0.029$). There were no differences between clonal and non-clonal cases in terms of the clinical and histological features such as age, tumor size, ER/HER2 status and type of LCIS.

Finally, in 4 patients, we analyzed triplets of 2 LCIS and 1 ILC from the same breast. In case #10, all 3 lesions shared 3 common mutations (*CDH1*, *PIK3CA* and *CBFB*), and also in case #13 we identified 2 common mutations (*CDH1* and *PKHD1L1*) in the 3 lesions (Figure 3). In case #48, however, LCIS-1 and ILC (located in the same upper outer quadrant) shared a common *CDH1* mutation, which was not present in LCIS-2, located in the upper inner quadrant of the same breast (Figure 3). In case #24, different foci of LCIS harbored distinct mutations affecting the same genes (Figure 3); whilst LCIS-1 and the ILC, which were located in the right lower outer quadrant, shared the same somatic mutations in *CDH1* (F730fs), *PIK3CA* (H1047R) and *CBFB* (Q67H); the LCIS-2, which was harvested from the upper inner quadrant of the same breast, harbored mutations in *CDH1* (Q23*) and *PIK3CA* (Q546R) distinct from those found in the LCIS-1 and ILC, providing an example of a convergent phenotype in the development of LCIS.

4. Discussion

Patients with LCIS have an increased risk of breast cancer that is 8- to 10-fold higher than the general population; yet the pathogenesis of this increased risk is poorly understood (Bratthauer and Tavassoli, 2002; Page et al., 1991). Morphologic and cytologic similarities between LCIS and ILC, combined with emerging reports of shared genomic alterations (mainly 1q gain, 16q loss and *CDH1* mutations) between LCIS and synchronous ILC have reopened the debate about the precursor potential of LCIS (Dabbs et al., 2013; Hwang et al., 2004; Mastracci et al., 2006; Vos et al., 1997); however, most studies have been limited to a small number of cases and based on formalin-fixed paraffin-embedded samples. Here, using fresh-frozen tissue samples from 30 patients and a targeted massively sequencing approach, we provide evidence in favor of the hypothesis that LCIS is a non-obligate precursor lesion to invasive disease. In addition, we demonstrate that targeted capture massively parallel sequencing can be used to assess clonal relatedness between

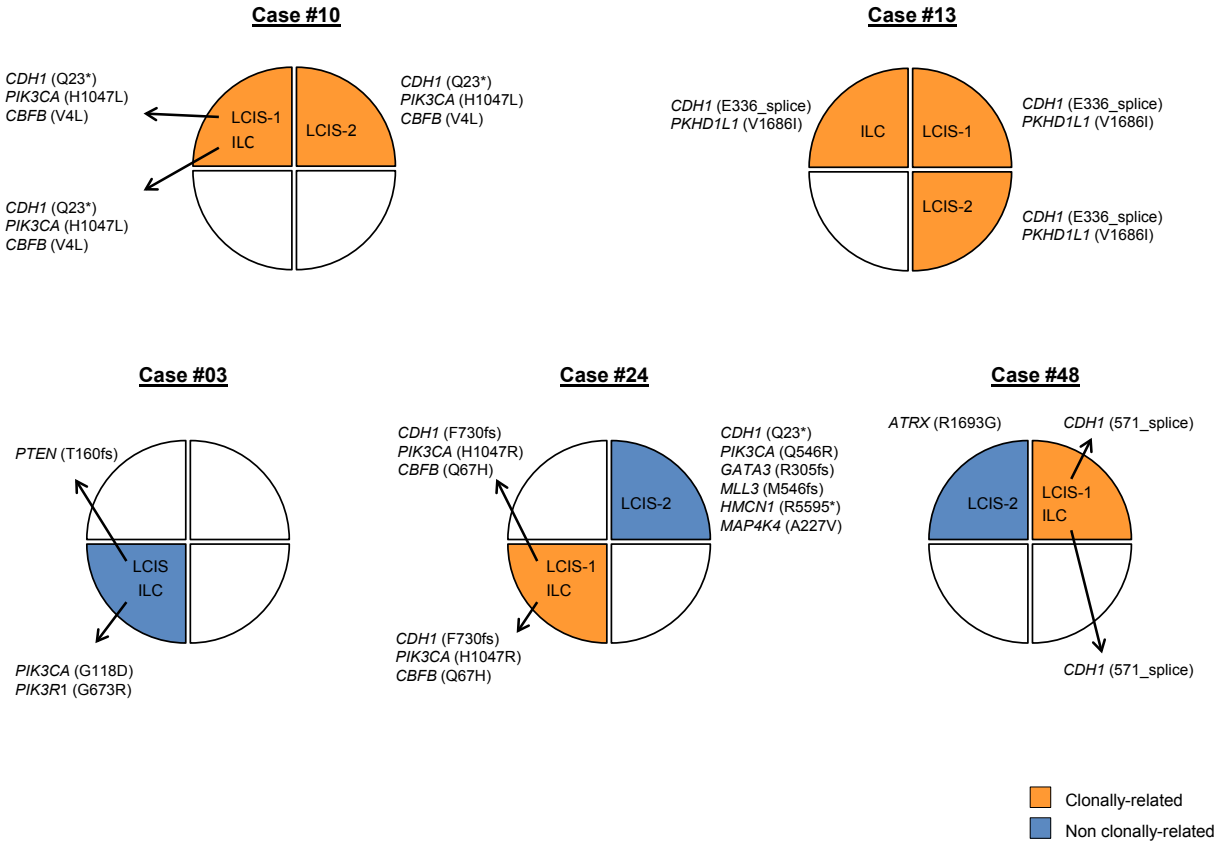

Figure 3 – Clonal relatedness between LCIS and ILC. Representation of the anatomical locations/breast quadrants of samples subjected to targeted massively parallel sequencing from cases for which three lesions (i.e., LCIS–LCIS–ILC) were analyzed or for cases where distinct somatic mutations between lesions were found. Clonally related lesions are indicated in orange, lesions in blue represent those without clonal relationship with any other lesion from the patient. ILC, invasive lobular cancer; LCIS, lobular carcinoma *in situ*.

synchronous LCIS and ILC lesions. Taken together, our results demonstrate that LCIS is a non-invasive neoplastic lesion that displays a constellation of somatic mutations strikingly similar to that of ILC. Furthermore, our data provide evidence to suggest that LCIS is often clonally related to synchronous ILC, and anatomically, seemingly independent foci of LCIS harvested from the same breast may be clonally related.

In addition to the unique morphologic and cytologic description of the lobular phenotype, loss of E-cadherin protein expression has long been recognized as a hallmark feature of lobular disease (Dabbs et al., 2013; Foote and Stewart, 1941; Haagensen et al., 1978). Loss of E-cadherin expression is reported to occur through a combination of mechanisms including *CDH1* gene mutation, allelic loss and *CDH1* promoter methylation (Droufakou et al., 2001; Lopez-Garcia et al., 2010). Here we confirm that genomic alterations affecting *CDH1* are an early event in lobular neoplasia with *CDH1* gene mutations observed in 58% and 64% of LCIS and ILC lesions, respectively (Table 2, Figure 1). Further, there was no significant difference in the pattern of *CDH1* mutations between LCIS and ILC samples. Previous studies with smaller sample sizes and different methodology have reported a higher frequency of CDH1 mutations in ILC (Logan et al., 2015); however, our findings are consistent with that of the most recent publication from The Cancer Genome Atlas Project, where *CDH1* mutations were identified in 63% (80/127) of classic invasive lobular carcinomas (Ciriello et al., 2014, 2015).

Mutations in *PIK3CA* were the second-most frequent mutations in both LCIS and ILC with a mutation frequency of 39% and 55%, respectively (Table 2, Figure 1), which is also consistent with the frequency of *PIK3CA* mutations reported in ER-positive breast cancer and ILC specifically (Cancer Genome Atlas, 2012; Saal et al., 2005; Stemke-Hale et al., 2008). The *CBFB* gene, which, like *CDH1*, is located on chromosome 16, was also recurrently mutated in our sample set of LCIS and ILC with a mutational frequency of 11% and 23%, respectively (Table 2, Figure 1). The comparison of the mutational frequency of *PIK3CA* mutations in our dataset of ILC with that of luminal A ER-positive invasive carcinomas or the lobular TCGA dataset (Cancer Genome Atlas, 2012) revealed no significant difference. In contrast, mutations in *CDH1* and *CBFB* were more frequent in ILCs in our dataset as compared to the luminal A ER-positive subtype from the TCGA dataset ($p < 0.0001$). The increased prevalence of *CDH1* mutations among lobular lesions is not unexpected and was confirmed in the TCGA lobular dataset (Ciriello et al., 2015). The enrichment in mutations targeting *CBFB* in ILCs in our dataset, however, warrants further validation.

In a smaller study presented by our group, which included an independent cohort of patients with LCIS, *CDH1* and *PIK3CA* were also found to be the most recurrently mutated genes in LCIS (De Brot et al., 2012). In this independent cohort, 36.4% (8/22) and 27.3% (6/22) of LCIS samples harbored *PIK3CA* and *CDH1* mutations, respectively (De Brot et al., 2012), which is similar to the mutation frequencies identified in the current series (*PIK3CA*, Fisher's exact test, two-tailed, $p = 0.785$; *CDH1*, Fisher's exact test, two-tailed, $p = 0.054$).

Different methodologies have been used in the literature to assess clonal relatedness between LCIS and adjacent malignancies including ILC, yet most are based on the analysis of gene copy number alterations in formalin-fixed paraffin-embedded samples (Hwang et al., 2004; Morandi et al., 2006; Wagner et al., 2009), or on the presence of identical *CDH1* mutations (Berx et al., 1996; De Leeuw et al., 1997; Droufakou et al., 2001; Rieger-Christ et al., 2001). One of the most frequently cited studies reporting the presence of shared mutations in LCIS and ILC included only 2 sets of paired lesions with common point mutations in the *CDH1* gene (Vos et al., 1997 #1}. Nonetheless, given that *CDH1* mutations in ILC do not occur at hotspots but at different residues within the gene, their specificity makes *CDH1* highly informative when assessing clonal relatedness. In the current study, we used fresh-frozen samples of both LCIS and ILC lesions prospectively harvested from all quadrants of the breast and subjected them to targeted capture massively parallel sequencing. Common mutations observed in both lesions of LCIS-ILC pairs support a likely clonal relationship in 71% of cases, with paired lesions being in the same quadrant of the breast in 12/15 (80%) cases and the repertoire of shared mutations including either one or both of the most recurrently mutated genes *CDH1* and *PIK3CA* (Table 3).

A limitation of our current study analysis was our inability to determine clonal relationship based on mutational data in 10% of LCIS-ILC pairs given the absence of mutations detected in one or both components of these pairs. Although targeted capture massively parallel sequencing allows a deeper sequencing coverage with lesser amounts of input DNA, it is limited to a panel of genes, and it is possible that our panel may not have included all of the genes relevant in the pathogenesis of LCIS or in the transition from LCIS to ILC. In addition, the small sample size reported here reflects the difficulty in harvesting fresh-frozen LCIS suitable for genomic analysis.

In conclusion, LCIS and ILC have a similar repertoire of somatic mutations, with *PIK3CA* and *CDH1* being the most frequently mutated genes. The presence of identical mutations between LCIS-LCIS and LCIS-ILC pairs demonstrates that LCIS is a clonal neoplastic lesion and provides additional data that LCIS is a non-obligate precursor of ILC. Further, we demonstrate that targeted capture massively parallel sequencing can be used to assess clonal relatedness between paired lesions.

Conflicts of interest

The authors have no conflicts of interest to declare.

Acknowledgment

S. Piscuoglio is funded by a Susan G Komen Postdoctoral Fellowship Grant (PDF14298348). Research reported in this study was supported in part by the Cancer Center Support Grant of the National Institutes of Health/National Cancer Institute under award number P30CA008748. The content is solely the responsibility of the authors and does not necessarily represent the official views of the National Institutes of Health. We acknowledge funding from Cycle for Survival, and the Marie-Josée and Henry R. Kravis Center for Molecular Oncology. The findings presented here were presented at the AACR annual meeting 2014, and have not been published elsewhere.

Appendix A. Supplementary data

Supplementary data related to this article can be found at http://dx.doi.org/10.1016/j.molonc.2015.11.001.

REFERENCES

Andrade, V.P., Ostrovnaya, I., Seshan, V.E., Morrogh, M., Giri, D., Olvera, N., De Brot, M., Morrow, M., Begg, C.B., King, T.A., 2012. Clonal relatedness between lobular carcinoma in situ and synchronous malignant lesions. Breast Cancer Res. 14, R103.

Banerji, S., Cibulskis, K., Rangel-Escareno, C., Brown, K.K., Carter, S.L., Frederick, A.M., Lawrence, M.S., Sivachenko, A.Y., Sougnez, C., Zou, L., Cortes, M.L., Fernandez-Lopez, J.C., Peng, S., Ardlie, K.G., Auclair, D., Bautista-Pina, V., Duke, F., Francis, J., Jung, J., Maffuz-Aziz, A., Onofrio, R.C., Parkin, M., Pho, N.H., Quintanar-Jurado, V., Ramos, A.H., Rebollar-Vega, R., Rodriguez-Cuevas, S., Romero-Cordoba, S.L., Schumacher, S.E., Stransky, N., Thompson, K.M., Uribe-Figueroa, L., Baselga, J., Beroukhim, R., Polyak, K., Sgroi, D.C., Richardson, A.L., Jimenez-Sanchez, G., Lander, E.S., Gabriel, S.B., Garraway, L.A., Golub, T.R., Melendez-Zajgla, J., Toker, A., Getz, G., Hidalgo-Miranda, A., Meyerson, M., 2012. Sequence analysis of mutations and translocations across breast cancer subtypes. Nature 486, 405–409.

Berx, G., Cleton-Jansen, A.M., Strumane, K., de Leeuw, W.J., Nollet, F., van Roy, F., Cornelisse, C., 1996. E-cadherin is inactivated in a majority of invasive human lobular breast cancers by truncation mutations throughout its extracellular domain. Oncogene 13, 1919–1925.

Bratthauer, G.L., Tavassoli, F.A., 2002. Lobular intraepithelial neoplasia: previously unexplored aspects assessed in 775 cases and their clinical implications. Virchows Archiv. 440, 134–138.

Cancer Genome Atlas Network, 2012. Comprehensive molecular portraits of human breast tumours. Nature 490, 61–70.

Carter, H., Chen, S., Isik, L., Tyekucheva, S., Velculescu, V.E., Kinzler, K.W., Vogelstein, B., Karchin, R., 2009. Cancer-specific high-throughput annotation of somatic mutations: computational prediction of driver missense mutations. Cancer Res. 69, 6660–6667.

Chandarlapaty, S., Sakr, R.A., Giri, D., Patil, S., Heguy, A., Morrow, M., Modi, S., Norton, L., Rosen, N., Hudis, C.,

King, T.A., 2012. Frequent mutational activation of the PI3K-AKT pathway in trastuzumab-resistant breast cancer. Clin. Cancer Res. 18, 6784–6791.
Cheng, D.T., Mitchell, T.N., Zehir, A., Shah, R.H., Benayed, R., Syed, A., Chandramohan, R., Liu, Z.Y., Won, H.H., Scott, S.N., Brannon, A.R., O'Reilly, C., Sadowska, J., Casanova, J., Yannes, A., Hechtman, J.F., Yao, J., Song, W., Ross, D.S., Oultache, A., Dogan, S., Borsu, L., Hameed, M., Nafa, K., Arcila, M.E., Ladanyi, M., Berger, M.F., 2015. Memorial Sloan Kettering-Integrated Mutation Profiling of Actionable Cancer Targets (MSK-IMPACT): a hybridization capture-based next-generation sequencing clinical assay for solid tumor molecular oncology. The J. Mol. Diagn. 17, 251–264.
Choi, Y., Sims, G.E., Murphy, S., Miller, J.R., Chan, A.P., 2012. Predicting the functional effect of amino acid substitutions and indels. PloS one 7, e46688.
Cibulskis, K., Lawrence, M.S., Carter, S.L., Sivachenko, A., Jaffe, D., Sougnez, C., Gabriel, S., Meyerson, M., Lander, E.S., Getz, G., 2013. Sensitive detection of somatic point mutations in impure and heterogeneous cancer samples. Nat. Biotechnol. 31, 213–219.
Ciriello, G., Gatza, M.L., Hoadley, K.A., Zhang, H., Rhie, S.K., Bowlby, R., Wilkerson, M.D., Kandoth, C., McLellan, M., Cherniack, A., Laird, P.W., Sander, C., King, T.A., Perou, C.M., 2014. Abstract S2-04: Comprehensive molecular characterization of invasive lobular breast tumors. Cancer Res. 75, S2–S04.
Ciriello, G., Gatza, M.L., Beck, A.H., Wilkerson, M.D., Rhie, S.K., Pastore, A., Zhang, H., McLellan, M., Yau, C., Kandoth, C., Bowlby, R., Shen, H., Hayat, S., Fieldhouse, R., Lester, S.C., Tse, G.M.K., Factor, R.E., Collins, L.C., Allison, K.H., Chen, Y.Y., Jensen, K., Johnson, N.B., Oesterreich, S., Mills, G.B., Cherniack, A.D., Robertson, G., Benz, C., Sander, C., Laird, P.W., Perou, C.M., 2015. Comprehensive molecular portraits of invasive lobular breast cancer. Cell 163, 506–519.
Dabbs, D.J., Schnitt, S.J., Geyer, F.C., Weigelt, B., Baehner, F.L., Decker, T., Eusebi, V., Fox, S.B., Ichihara, S., Lakhani, S.R., Palacios, J., Rakha, E., Richardson, A.L., Schmitt, F.C., Tan, P.H., Tse, G.M., Vincent-Salomon, A., Ellis, I.O., Badve, S., Reis-Filho, J.S., 2013. Lobular neoplasia of the breast revisited with emphasis on the role of E-cadherin immunohistochemistry. Am. J. Surg. Pathol. 37, e1–11.
De Brot, M., Andrade, V.P., Morrogh, M., Berger, M.F., Won, H.H., Koslow, M.S., Qin, L.-X., Giri, D.D., Olvera, N., Sakr, R.A., King, T.A., 2012. Novel Mutations in Lobular Carcinoma in Situ (LCIS) as Uncovered by Targeted Parallel sequencing., Thirty-fifth Annual CTRC-AACR San Antonio Breast Cancer Symposium. Cancer Res, San Antonio, TX pp. Abstract nr PD05–02.
De Leeuw, W.J., Berx, G., Vos, C.B., Peterse, J.L., Van de Vijver, M.J., Litvinov, S., Van Roy, F., Cornelisse, C.J., Cleton-Jansen, A.M., 1997. Simultaneous loss of E-cadherin and catenins in invasive lobular breast cancer and lobular carcinoma in situ. J. Pathol. 183, 404–411.
Ding, J., Bashashati, A., Roth, A., Oloumi, A., Tse, K., Zeng, T., Haffari, G., Hirst, M., Marra, M.A., Condon, A., Aparicio, S., Shah, S.P., 2012. Feature-based classifiers for somatic mutation detection in tumour-normal paired sequencing data. Bioinformatics 28, 167–175.
Droufakou, S., Deshmane, V., Roylance, R., Hanby, A., Tomlinson, I., Hart, I.R., 2001. Multiple ways of silencing E-cadherin gene expression in lobular carcinoma of the breast. Int. j. Cancer 92, 404–408.
Ellis, M.J., Ding, L., Shen, D., Luo, J., Suman, V.J., Wallis, J.W., Van Tine, B.A., Hoog, J., Goiffon, R.J., Goldstein, T.C., Ng, S., Lin, L., Crowder, R., Snider, J., Ballman, K., Weber, J., Chen, K., Koboldt, D.C., Kandoth, C., Schierding, W.S., McMichael, J.F., Miller, C.A., Lu, C., Harris, C.C., McLellan, M.D., Wendl, M.C., DeSchryver, K., Allred, D.C., Esserman, L., Unzeitig, G., Margenthaler, J., Babiera, G.V., Marcom, P.K., Guenther, J.M., Leitch, M., Hunt, K., Olson, J., Tao, Y., Maher, C.A., Fulton, L.L., Fulton, R.S., Harrison, M., Oberkfell, B., Du, F., Demeter, R., Vickery, T.L., Elhammali, A., Piwnica-Worms, H., McDonald, S., Watson, M., Dooling, D.J., Ota, D., Chang, L.W., Bose, R., Ley, T.J., Piwnica-Worms, D., Stuart, J.M., Wilson, R.K., Mardis, E.R., 2012. Whole-genome analysis informs breast cancer response to aromatase inhibition. Nature 486, 353–360.
Foote, F.W., Stewart, F.W., 1941. Lobular carcinoma in situ: a rare form of mammary cancer. Am. J. Pathol. 17, 491–496 493.
Futreal, P.A., Coin, L., Marshall, M., Down, T., Hubbard, T., Wooster, R., Rahman, N., Stratton, M.R., 2004. A census of human cancer genes. Nat. Rev. Cancer 4, 177–183.
Gao, J., Aksoy, B.A., Dogrusoz, U., Dresdner, G., Gross, B., Sumer, S.O., Sun, Y., Jacobsen, A., Sinha, R., Larsson, E., Cerami, E., Sander, C., Schultz, N., 2013. Integrative analysis of complex cancer genomics and clinical profiles using the cBioPortal. Sci. Signal. 6, pl1.
Haagensen, C.D., Lane, N., Lattes, R., Bodian, C., 1978. Lobular neoplasia (so-called lobular carcinoma in situ) of the breast. Cancer 42, 737–769.
Hwang, E.S., Nyante, S.J., Yi Chen, Y., Moore, D., DeVries, S., Korkola, J.E., Esserman, L.J., Waldman, F.M., 2004. Clonality of lobular carcinoma in situ and synchronous invasive lobular carcinoma. Cancer 100, 2562–2572.
Kandoth, C., McLellan, M.D., Vandin, F., Ye, K., Niu, B., Lu, C., Xie, M., Zhang, Q., McMichael, J.F., Wyczalkowski, M.A., Leiserson, M.D., Miller, C.A., Welch, J.S., Walter, M.J., Wendl, M.C., Ley, T.J., Wilson, R.K., Raphael, B.J., Ding, L., 2013. Mutational landscape and significance across 12 major cancer types. Nature 502, 333–339.
Koboldt, D.C., Zhang, Q., Larson, D.E., Shen, D., McLellan, M.D., Lin, L., Miller, C.A., Mardis, E.R., Ding, L., Wilson, R.K., 2012. VarScan 2: somatic mutation and copy number alteration discovery in cancer by exome sequencing. Genome Res. 22, 568–576.
Lakhani, S.R., Ellis, I.O., Schnitt, S.J., Tan, P.H., van de Vijver, M.J. (Eds.), 2012. WHO Classification of Breast Tumors. IARC, Lyon.
Lakhani, S.R., Audretsch, W., Cleton-Jensen, A.M., Cutuli, B., Ellis, I., Eusebi, V., Greco, M., Houslton, R.S., Kuhl, C.K., Kurtz, J., Palacios, J., Peterse, H., Rochard, F., Rutgers, E., Eusoma, 2006. The management of lobular carcinoma in situ (LCIS). Is LCIS the same as ductal carcinoma in situ (DCIS)? Eur. J. Cancer 42, 2205–2211.
Lakhani, S.R., Collins, N., Sloane, J.P., Stratton, M.R., 1995. Loss of heterozygosity in lobular carcinoma in situ of the breast. Clin. Mol. Pathol. 48, M74–M78.
Larson, D.E., Harris, C.C., Chen, K., Koboldt, D.C., Abbott, T.E., Dooling, D.J., Ley, T.J., Mardis, E.R., Wilson, R.K., Ding, L., 2012. SomaticSniper: identification of somatic point mutations in whole genome sequencing data. Bioinformatics 28, 311–317.
Lawrence, M.S., Stojanov, P., Mermel, C.H., Robinson, J.T., Garraway, L.A., Golub, T.R., Meyerson, M., Gabriel, S.B., Lander, E.S., Getz, G., 2014. Discovery and saturation analysis of cancer genes across 21 tumour types. Nature 505, 495–501.
Li, H., Durbin, R., 2009. Fast and accurate short read alignment with Burrows-Wheeler transform. Bioinformatics 25, 1754–1760.
Logan, G.J., Dabbs, D.J., Lucas, P.C., Jankowitz, R.C., Brown, D.D., Clark, B.Z., Oesterreich, S., McAuliffe, P.F., 2015. Molecular drivers of lobular carcinoma in situ. Breast Cancer Res. 17, 76.
Lopez-Garcia, M.A., Geyer, F.C., Lacroix-Triki, M., Marchio, C., Reis-Filho, J.S., 2010. Breast cancer precursors revisited: molecular features and progression pathways. Histopathology 57, 171–192.

Martelotto, L.G., Ng, C., De Filippo, M.R., Zhang, Y., Piscuoglio, S., Lim, R., Shen, R., Norton, L., Reis-Filho, J.S., Weigelt, B., 2014. Benchmarking mutation effect prediction algorithms using functionally validated cancer-related missense mutations. Genome Biol. 15, 484.

Mastracci, T.L., Shadeo, A., Colby, S.M., Tuck, A.B., O'Malley, F.P., Bull, S.B., Lam, W.L., Andrulis, I.L., 2006. Genomic alterations in lobular neoplasia: a microarray comparative genomic hybridization signature for early neoplastic proliferationin the breast. Genes chromosomes cancer 45, 1007–1017.

McKenna, A., Hanna, M., Banks, E., Sivachenko, A., Cibulskis, K., Kernytsky, A., Garimella, K., Altshuler, D., Gabriel, S., Daly, M., DePristo, M.A., 2010. The Genome Analysis Toolkit: a MapReduce framework for analyzing next-generation DNA sequencing data. Genome Res. 20, 1297–1303.

Morandi, L., Marucci, G., Foschini, M.P., Cattani, M.G., Pession, A., Riva, C., Eusebi, V., 2006. Genetic similarities and differences between lobular in situ neoplasia (LN) and invasive lobular carcinoma of the breast. Virchows Arch. 449, 14–23.

Natrajan, R., Wilkerson, P.M., Marchio, C., Piscuoglio, S., Ng, C.K., Wai, P., Lambros, M.B., Samartzis, E.P., Dedes, K.J., Frankum, J., Bajrami, I., Kopec, A., Mackay, A., A'Hern, R., Fenwick, K., Kozarewa, I., Hakas, J., Mitsopoulos, C., Hardisson, D., Lord, C.J., Kumar-Sinha, C., Ashworth, A., Weigelt, B., Sapino, A., Chinnaiyan, A.M., Maher, C.A., Reis-Filho, J.S., 2014. Characterization of the genomic features and expressed fusion genes in micropapillary carcinomas of the breast. J. Pathol. 232, 553–565.

Page, D.L., Kidd Jr., T.E., Dupont, W.D., Simpson, J.F., Rogers, L.W., 1991. Lobular neoplasia of the breast: higher risk for subsequent invasive cancer predicted by more extensive disease. Hum. Pathol. 22, 1232–1239.

Rieger-Christ, K.M., Pezza, J.A., Dugan, J.M., Braasch, J.W., Hughes, K.S., Summerhayes, I.C., 2001. Disparate E-cadherin mutations in LCIS and associated invasive breast carcinomas. Mol. Pathol. 54, 91–97.

Robinson, J.T., Thorvaldsdottir, H., Winckler, W., Guttman, M., Lander, E.S., Getz, G., Mesirov, J.P., 2011. Integrative genomics viewer. Nat. Biotechnol. 29, 24–26.

Saal, L.H., Holm, K., Maurer, M., Memeo, L., Su, T., Wang, X., Yu, J.S., Malmstrom, P.O., Mansukhani, M., Enoksson, J., Hibshoosh, H., Borg, A., Parsons, R., 2005. PIK3CA mutations correlate with hormone receptors, node metastasis, and ERBB2, and are mutually exclusive with PTEN loss in human breast carcinoma. Cancer Res. 65, 2554–2559.

Sakr, R.A., Weigelt, B., Chandarlapaty, S., Andrade, V.P., Guerini-Rocco, E., Giri, D., Ng, C.K., Cowell, C.F., Rosen, N., Reis-Filho, J.S., King, T.A., 2014. PI3K pathway activation in high-grade ductal carcinoma in situ–implications for progression to invasive breast carcinoma. Clin. Cancer Res. 20, 2326–2337.

Schwarz, J.M., Rodelsperger, C., Schuelke, M., Seelow, D., 2010. MutationTaster evaluates disease-causing potential of sequence alterations. Nat. Methods 7, 575–576.

Shihab, H.A., Gough, J., Cooper, D.N., Stenson, P.D., Barker, G.L., Edwards, K.J., Day, I.N., Gaunt, T.R., 2013. Predicting the functional, molecular, and phenotypic consequences of amino acid substitutions using hidden Markov models. Hum. Mutat. 34, 57–65.

Stemke-Hale, K., Gonzalez-Angulo, A.M., Lluch, A., Neve, R.M., Kuo, W.L., Davies, M., Carey, M., Hu, Z., Guan, Y., Sahin, A., Symmans, W.F., Pusztai, L., Nolden, L.K., Horlings, H., Berns, K., Hung, M.C., van de Vijver, M.J., Valero, V., Gray, J.W., Bernards, R., Mills, G.B., Hennessy, B.T., 2008. An integrative genomic and proteomic analysis of PIK3CA, PTEN, and AKT mutations in breast cancer. Cancer Res. 68, 6084–6091.

Stephens, P.J., Tarpey, P.S., Davies, H., Van Loo, P., Greenman, C., Wedge, D.C., Nik-Zainal, S., Martin, S., Varela, I., Bignell, G.R., Yates, L.R., Papaemmanuil, E., Beare, D., Butler, A., Cheverton, A., Gamble, J., Hinton, J., Jia, M., Jayakumar, A., Jones, D., Latimer, C., Lau, K.W., McLaren, S., McBride, D.J., Menzies, A., Mudie, L., Raine, K., Rad, R., Chapman, M.S., Teague, J., Easton, D., Langerod, A., Oslo Breast Cancer, C., Lee, M.T., Shen, C.Y., Tee, B.T., Huimin, B.W., Broeks, A., Vargas, A.C., Turashvili, G., Martens, J., Fatima, A., Miron, P., Chin, S.F., Thomas, G., Boyault, S., Mariani, O., Lakhani, S.R., van de Vijver, M., van 't Veer, L., Foekens, J., Desmedt, C., Sotiriou, C., Tutt, A., Caldas, C., Reis-Filho, J.S., Aparicio, S.A., Salomon, A.V., Borresen-Dale, A.L., Richardson, A.L., Campbell, P.J., Futreal, P.A., Stratton, M.R., 2012. The landscape of cancer genes and mutational processes in breast cancer. Nature 486, 400–404.

Vos, C.B., Cleton-Jansen, A.M., Berx, G., de Leeuw, W.J., ter Haar, N.T., van Roy, F., Cornelisse, C.J., Peterse, J.L., van de Vijver, M.J., 1997. E-cadherin inactivation in lobular carcinoma in situ of the breast: an early event in tumorigenesis. Br. J. Cancer 76, 1131–1133.

Wagle, N., Berger, M.F., Davis, M.J., Blumenstiel, B., Defelice, M., Pochanard, P., Ducar, M., Van Hummelen, P., Macconaill, L.E., Hahn, W.C., Meyerson, M., Gabriel, S.B., Garraway, L.A., 2012. High-throughput detection of actionable genomic alterations in clinical tumor samples by targeted, massively parallel sequencing. Cancer Discov. 2, 82–93.

Wagner, P.L., Kitabayashi, N., Chen, Y.T., Shin, S.J., 2009. Clonal relationship between closely approximated low-grade ductal and lobular lesions in the breast: a molecular study of 10 cases. Am. J. Clin. Pathol. 132, 871–876.

Weinreb, I., Piscuoglio, S., Martelotto, L.G., Waggott, D., Ng, C.K., Perez-Ordonez, B., Harding, N.J., Alfaro, J., Chu, K.C., Viale, A., Fusco, N., da Cruz Paula, A., Marchio, C., Sakr, R.A., Lim, R., Thompson, L.D., Chiosea, S.I., Seethala, R.R., Skalova, A., Stelow, E.B., Fonseca, I., Assaad, A., How, C., Wang, J., de Borja, R., Chan-Seng-Yue, M., Howlett, C.J., Nichols, A.C., Wen, Y.H., Katabi, N., Buchner, N., Mullen, L., Kislinger, T., Wouters, B.G., Liu, F.F., Norton, L., McPherson, J.D., Rubin, B.P., Clarke, B.A., Weigelt, B., Boutros, P.C., Reis-Filho, J.S., 2014. Hotspot activating PRKD1 somatic mutations in polymorphous low-grade adenocarcinomas of the salivary glands. Nat. Genet. 46, 1166–1169.